SOLUTION OF EQUILIBRIUM PRANDTL-MEYER FLOW OF A REAL GAS BY THE METHOD OF EQUIVALENT IDEAL FLOW

Fang Toh Sun

Gas Dynamics Laboratories
Department of Aerospace Engineering
The University of Michigan
Ann Arbor, Michigan

June 1966

TABLE OF CONTENTS

ABSTRACT

A practical method for the solution of Prandtl-Meyer flow of a real gas in equilibrium is presented. The concept of an equivalent ideal flow is introduced and the exact solution of the Prandtl-Meyer flow of an ideal gas is utilized to reduce the bulk of graphical work needed for the solution of a real flow. A few typical key-charts for this method are developed for equilibrium air and from these charts the behavior of equilibrium air in a Prandtl-Meyer flow is briefly reviewed. Several numerical examples illustrating the application of this method are included in the appendix.

ACKNOWLEDGMENT

The author is grateful to The University of Michigan Institute of Science and Technology for its financial support of the work presented in this report. Special thanks are due to Prof. J. A. Nicholls, whose encouragement and support made this work possible. Thanks are also due to Messrs. Harry H. Watanabe and James Howe for their help in the tedious calculations and plotting.

LIST OF ILLUSTRATIONS

NOMENCLATURE

a	speed of sound
a^*	critical speed of sound
h	enthalpy per unit mass
M	Mach number, V/a
M^*	dimensionless velocity, V/a^*
p	pressure
r	radial distance
R	gas constant
s	entropy per unit mass
T	absolute temperature
V	speed
V_r	radial component of velocity
V_θ	transversal component of velocity
α	Mach angle
γ	ratio of specific heats, c_p/c_v
δ	deflection angle, defined in Fig. 1
θ	polar angle, defined in Fig. 1
ρ	density
λ	flow parameter $= \sqrt{1 + \frac{2h}{a^2}}$
$\bar{\lambda}$	average value of λ, defined by Eq. (C-1)

Subscripts

i	ideal flow
o	reference condition
s	isentropic
t	stagnation condition

I. INTRODUCTION

The problem of supersonic flow through a centered expansion wave, known as Prandtl-Meyer flow, has been solved analytically for the case of an ideal gas by L. Prandtl[1] and Th. Meyer[2] in the early nineteen hundreds, and hodographs and tables have been extensively developed since then[3, 4, 6, 7] However, when the real gas effects are to be taken into account (such as the variation of specific heats with temperature, dissociation, ionization, and so on), analytical solutions have not been available, and the solution of such problems has to rely heavily on numerical approximations and graphical means. As a great variety of real gases and flow conditions are encountered in present-day engineering, a tremendous amount of numerical and graphical work will be expected.

The purpose of this report is to solve the problem of Prandtl-Meyer flow of a real gas by correlating it with an equivalent ideal flow, a concept which will be introduced below. Through such a correlation it will be shown that the solution of the real flow problems may be obtained from that of an ideal flow, so that the existing analytical solution for the ideal case may be utilized, and the graphical and numerical work necessary for the real flow problems will be greatly reduced.

II. ANALYSIS

With the gas assumed in local thermodynamic equilibrium throughout its expansion around a convex sharp corner, it is expected that all physical properties of the gas will be constant along the radial lines emanating from the corner since the boundary conditions define no characteristic length in such a problem according to Prandtl's argument[1, 5] and the resulting flow is therefore of the Prandtl-Meyer type. Under such assumptions the flow is isentropic and the following equations hold not only for an ideal gas but for a real gas as well:

$$\frac{dV_r}{d\theta} = V_\theta = a \tag{1}$$

$$\frac{1}{2}\left(V_r^2 + V_\theta\right) = (h_t - h)_s \tag{2}$$

since they are based on the conservation of mass, momentum, and energy only, hence independent of the equation of state of the particular gas under consideration. The geometry of such a flow is shown in Fig. 1.

Eliminating V_θ from Eqs. (1) and (2) results in Heims' equation* for the radial velocity V_r,

---

*First introduced by Heims, Steve P. in Ref. 10 with a slightly different notation.

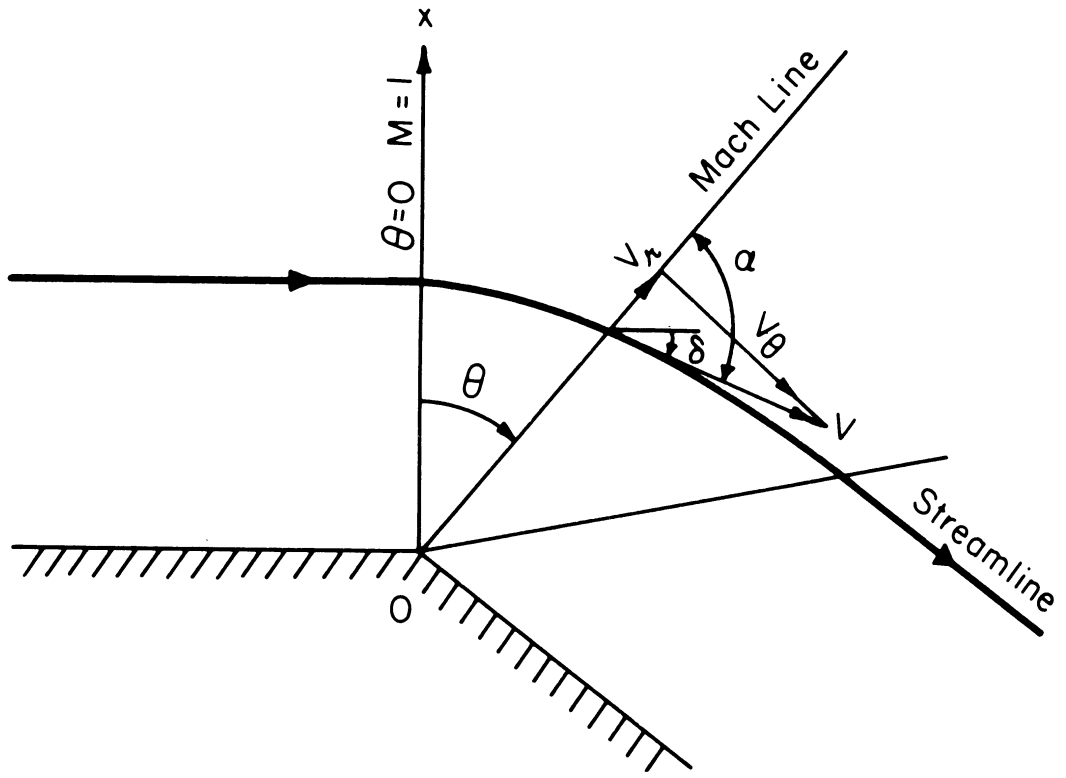

Figure 1. Geometry of the Prandtl - Meyer Flow

$$\left(\frac{dV_r}{d\theta}\right)^2 = \left[\frac{1}{\lambda^2}\left(2h_t - V_r^2\right)\right]_s \tag{3}$$

where the parameter λ is defined by

$$\lambda^2 \equiv 1 + \frac{2h}{a^2} \tag{4}$$

A comparison of Eq. (3) with the corresponding equation for an ideal gas,

$$\left(\frac{dV_{ri}}{d\theta_i}\right)^2 = \left[\frac{1}{\lambda_i^2}\left(2h_{ti} - V_{ri}^2\right)\right]_s \tag{3a}$$

with

$$\lambda_i^2 = 1 + \frac{2h_i}{a_i^2} = \frac{\gamma_i + 1}{\gamma_i - 1} \tag{4a}$$

suggests the following change of variable:

$$\frac{d\theta}{\lambda} = \frac{d\theta_i}{\lambda_i} \tag{5}$$

Upon substituting the new variable θ_i for θ, Eq. (3) reduces to

$$\left(\frac{dV_r}{d\theta_i}\right)^2 = \left[\frac{1}{\lambda_i^2}\left(2h_t - V_r^2\right)\right]_s \tag{6}$$

which is exactly of the same form as Eq. (3a). Thus, as a consequence of such a transformation, we arrive at

$$V_r = V_{ri} \tag{7}$$

if we take $h_{ti} = h_t$. That is, the radial velocity along the radial line of polar angle θ in the real flow is the same in magnitude as that in the flow of an ideal gas of the same stagnation enthalpy along the corresponding radial line of polar angle θ_i defined by Eq. (5). The fictitious flow of an ideal gas associated with a real gas flow in the sense of Eq. (7) will be referred to as the equivalent ideal Prandtl-Meyer flow (or ideal flow for short) wherein the polar angles of the corresponding radial lines along which the radial components of the gas velocities in the two flows are equal (in magnitude) are related through Eq. (5).

III. CORRELATION BETWEEN THE REAL FLOW AND THE IDEAL FLOW

With the basic correlation between the real Prandtl-Meyer flow and its equivalent ideal flow established in Eqs. (5) and (7) it is a simple matter to deduce the relations between other gas properties along the corresponding radial lines. For example, the corresponding transversal components of the flow velocities are related by

$$V_\theta = \frac{dV_r}{d\theta} = \frac{dV_r}{d\theta_i}\frac{d\theta_i}{d\theta} = \frac{\lambda_i}{\lambda} V_{\theta i} \tag{8}$$

The correlation between other properties may be deduced in the same manner. A summary of such formulas is given below:

Table 1. Correlation Between the Real and Ideal Prandtl-Meyer Flows

Flow Parameter	Correlation Formula	
Velocity, radial	$V_r = V_{ri}$	(7)
Velocity, transversal	$V_\theta = \left(\frac{\lambda_i}{\lambda}\right) V_{\theta i}$	(8)
Local speed of sound	$a = \left(\frac{\lambda_i}{\lambda}\right) a_i$	(9)
Mach angle	$\tan \alpha = \left(\frac{\lambda_i}{\lambda}\right) \tan \alpha_i$	(10)
Mach number	$M^2 = 1 + \left(\frac{\lambda}{\lambda_i}\right)^2 (M_i^2 - 1)$	(11)
Local enthalpy	$h = \left(\frac{1 - 1/\lambda^2}{1 - 1/\lambda_i^2}\right) h_i$	(12)

Thus once the correspondence between θ and θ_i is established, all principal flow parameters in the real flow can be obtained from the corresponding quantities in the equivalent ideal flow by simple calculations through these correlation formulas. (A summary of the analytical solution and a short table for the ideal flow will be found in Appendices A and B.)

So far no attempt has been made to correlate directly the corresponding local flow deflections δ and δ_i as it is more involved. However, with the polar angle θ and the local Mach angle α determined, the local deflection in the real flow may be simply calculated from

$$\delta = \theta + \alpha - \frac{\pi}{2} \tag{13}$$

which is evident from the geometry of the flow (see Fig. 1).

Now it remains to integrate the differential relation (5) between θ and θ_i. In the absence of suitable analytical formulas the integration can only be effected graphically. Before proceeding with such an integration we recall from the analytic solution for an ideal Prandtl-Meyer flow,

$$a_i = V_{\theta i} = \frac{1}{\lambda_i} \sqrt{2h_t} \cos (\theta_i/\lambda_i) \tag{14}$$

which when,combined with the correlation formula (9), gives

$$\theta_i = \lambda_i \cos^{-1} \frac{\lambda a}{\sqrt{2h_t}} \tag{15}$$

This equation provides a principal linkage between the condition in the real flow and the corresponding polar angle in the ideal flow, and enables one to effect the integration of Eq. (5) according to the procedure suggested below.

For a specified stagnation condition defined by h_t and s,

1) Assume a series of values of local enthalpy, $h < h_t$ along the constant entropy line, and find the corresponding local speed of sound from the proper chart (e. g. , the Mollier chart) or table for the real gas under consideration;

2) Calculate λ according to Eq. (4) and then θ_i according to Eq. (15):

3) Plot λ versus θ_i and carry out the graphical integration according to

$$\theta = \int_0^{\theta_i} \frac{\lambda}{\lambda_i} \, d\theta_i \tag{5a}$$

It is to be noted that both θ and θ_i are measured from the Mach line M = 1 by definition; and in principle, any ideal gas, monatomic or polyatomic, may be taken as the reference gas in the ideal flow irrespective of the nature of the real gas under consideration.

As an illustration, some typical correlation charts for θ and θ_i, δ and δ_i have been worked out for equilibrium air by the present method with a diatomic gas as the reference gas. The results together with the λ vs. θ_i curves from which these correlation charts were obtained are shown in Figs. 2 to 4. Some typical examples showing the use of these charts for the solution of practical problems are given in Appendix D.

As further illustrations, the variation of the local properties of equilibrium air (temperature ratio, pressure ratio, density ratio, and Mach number) through the Prandtl-Meyer expansion as obtained from these basic charts are presented in Figs. 5 to 8. The corresponding quantities for an ideal diatomic gas given by the analytical solution are also shown for comparison purpose.

IV. THE PRANDTL-MEYER FLOW OF EQUILIBRIUM AIR

Based on the graphs presented in Figs. 2 to 8, a few observations on the Prandtl-Meyer flow of equilibrium air may now be made.

The relation between the corresponding real and ideal polar angles is nearly linear at a constant stagnation condition. The slope of such a line $(d\theta/d\theta_i)$ changes in going from one isentropic line to another, the higher the entropy the higher the slope; but it remains practically constant for different stagnation enthalpy. This is due to the fact that the parameter λ of the real gas changes considerably with entropy but very little with enthalpy. With the help of the Mollier chart[9] the variation of λ with enthalpy and entropy for equilibrium air is shown in Fig. 9. An empirical formula for the average slope of the $\theta - \theta_i$ curve for equilibrium air is given in Appendix C.

A comparison of the equilibrium properties of air in a real flow with an ideal flow shows that, within the range of the present plots, the temperature ratio (T/T_t) in a real flow is higher than that in an ideal flow at the

same angle of deflection (both measured from the initial direction M = 1); and the same is true for the pressure ratio (p/p_o). The deviation of air temperature in the real flow from that in an ideal flow of the same stagnation temperature first increases and then decreases as the flow deflection increases, with the maximum deviation occurring at some intermediate deflection angle (Fig. 5). However, the pressure deviation between a real flow and an ideal flow of the same stagnation pressure is small, and is practically negligible at high flow deflections (Fig. 6).

In the case of density ratio, as Fig. 7 shows, the difference in the real and ideal flows is very little throughout the range of plotting. For small flow deflection the air density in the real flow is slightly lower than that in the ideal flow of the same stagnation density while for large deflection it is slightly higher. The two become identical at an intermediate flow deflection of approximately 38^o under the assumed stagnation condition.

Finally the Mach number in the real flow is lower than that in the ideal flow at the same turning angle, and this deviation increases rapidly as the air turns (Fig. 8). As we know, the maximum angle of turning in an ideal flow has a theoretical limit of $[\sqrt{(\gamma + 1)/(\gamma - 1)} - 1]\, \pi/2$, the present plotting indicates that the equilibrium air may turn through a much higher angle than an ideal diatomic gas.

V. DISCUSSION

1. As shown throughout the previous sections the parameter λ plays a vital role in the behavior of the Prandtl-Meyer type of gas flow. By writing its defining Eq. (4) in the alternate form

$$\lambda^2 = \frac{h + \frac{1}{2}a^2}{\frac{1}{2}a^2} \tag{4'}$$

it is seen that the square of λ represents the ratio of the total energy to the kinetic energy of the gas if the flow is critical, that is, $V = a$, under the local condition defined by its enthalpy and entropy. Heim's equation then shows that even though a great variety of real gas effects are present in the real flow, they enter the governing equation only through this parameter as long as the assumption of equilibrium flow is valid. Consequently, the introduction of this parameter provides a simple approach to the analysis of Prandtl-Meyer flow despite the presence of apparently many diversified real gas effects; and it also makes it possible to link the real gas flow with an ideal gas flow which forms the basis of the present method of solution.

A few typical curves showing the variation of λ with the local enthalpy and entropy have been presented in Fig. 9 for equilibrium air. In fact lines of constant λ may be added to a regular Mollier chart since it is a local property of the gas. Such Mollier charts, if available, would be of special value in assisting the solution of Prandtl-Meyer flow problems of real gases.

2. As Section III shows, by linking the real flow with its equivalent ideal flow through the parameter λ the problem of finding the solution for a real flow reduces to that for an ideal flow if the correspondence between the real and ideal polar angles θ and θ_i is known. Thus the graphical work necessary for such a solution is narrowed down to the graphical integration of the single relation $\lambda_i d\theta = \lambda d\theta_i$ from which the θ vs. θ_i charts may be prepared. Once such charts are available, the method of solution consists of merely finding the ideal solution according to θ_i and converting it to the real solution through the simple correlation formulas in the table of Section III.

Basically the θ vs. θ_i charts together with the λ vs. θ_i charts, constitute the key charts needed in the present method. However, in view of the fact that in many practical problems it is usually the local deflection angle that is specified instead of the polar angle, correlation charts of δ vs. δ_i such as those shown in Figs. 3-1 to 3-3 are often desired. Such charts may be easily obtained from the θ vs. θ_i chart through formula (13). Thus, by using the equivalent ideal flow method, at most three types of correlation charts are required; the θ vs. θ_i, δ vs. δ_i, and λ vs. θ_i; and to prepare these charts only one graphical integration is needed. In case of equilibrium air the empirical formula in Appendix C may be used in the absence of the θ vs. θ_i charts.

Finally it is to be noted that the graphical integration of the differential relation $\lambda_i d\theta = \lambda\theta_i$ on which the present method hinges can be effected only when the equilibrium properties of the real gas under consideration are known (either in the form of charts, tables, or empirical formulas). Investigations of such properties of various real gases are beyond the scope of the present study.

3. Although this report deals with the equilibrium flow, same method applies equally to the case of frozen flow. In such a case the value of λ is frozen at its initial value and the real gas behaves as an ideal gas throughout the flow. Consequently, the θ vs. θ_i relation is exactly linear, and a direct application of ideal flow formulas is permitted with a proper choice of the value of λ.

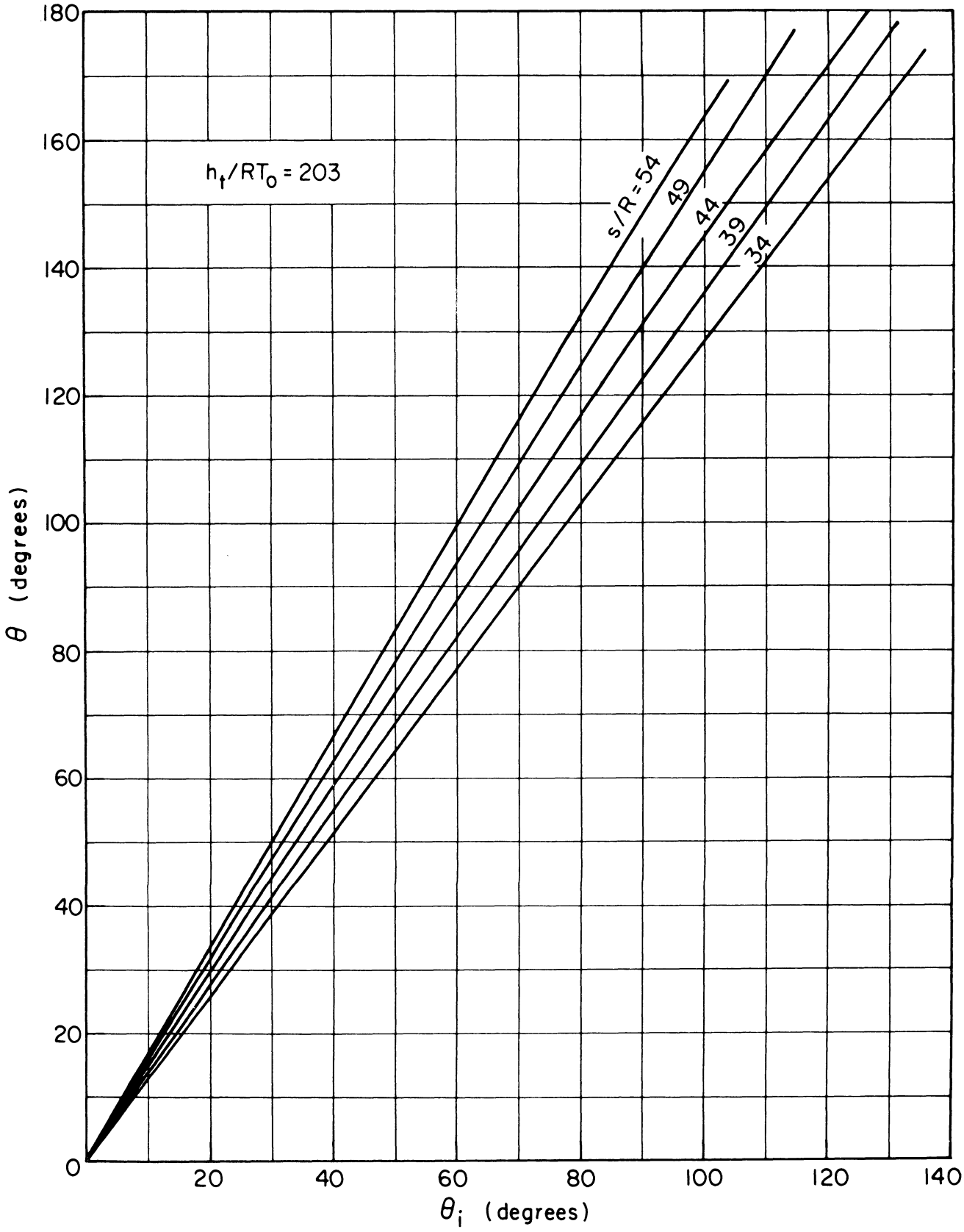

Figure 2-1. Correlation Chart A: θ vs. θ_i ($h_t/RT_0 = 203$)

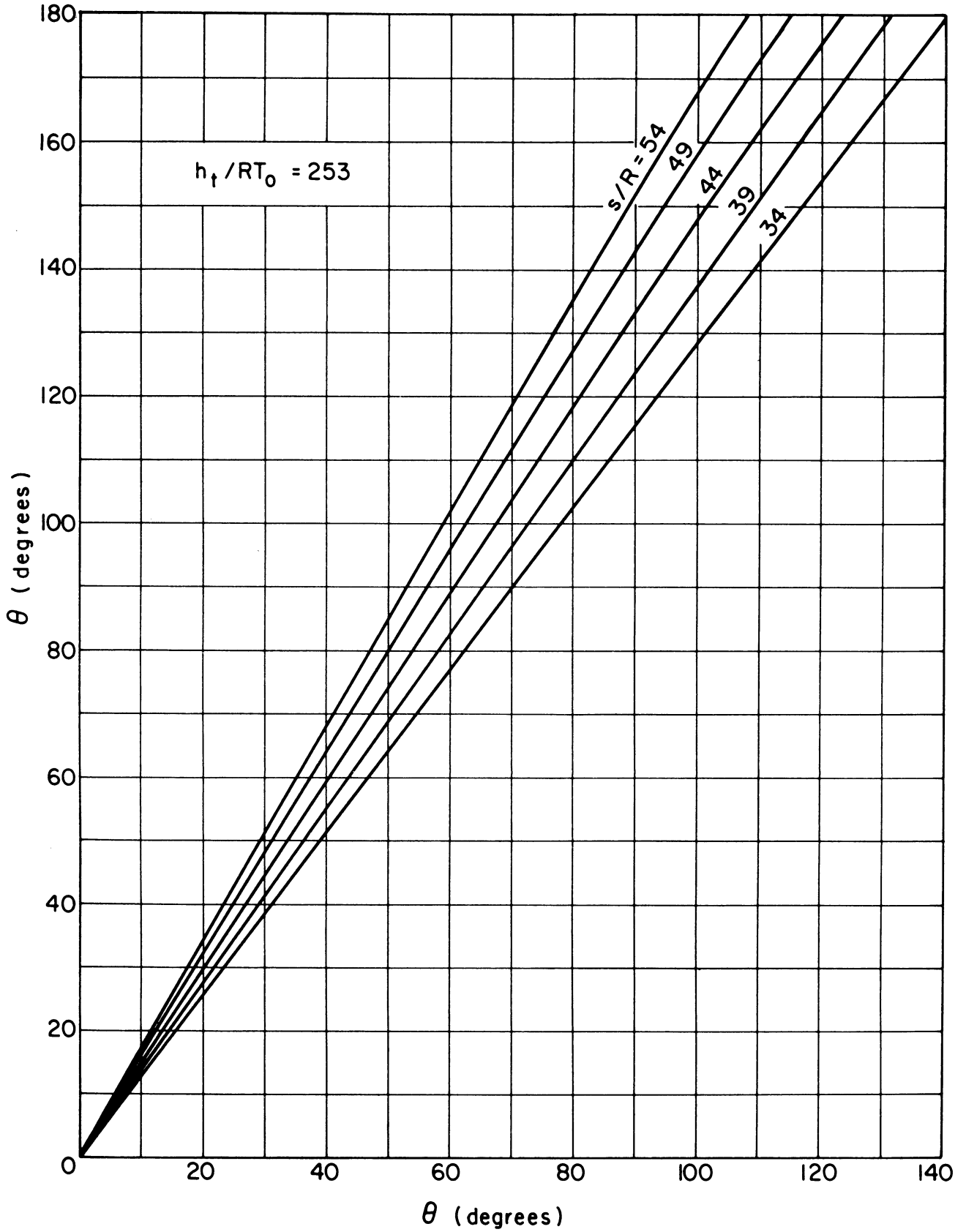

Figure 2-2. Correlation Chart A: θ vs. θ_i (h_t/RT_0 = 253)

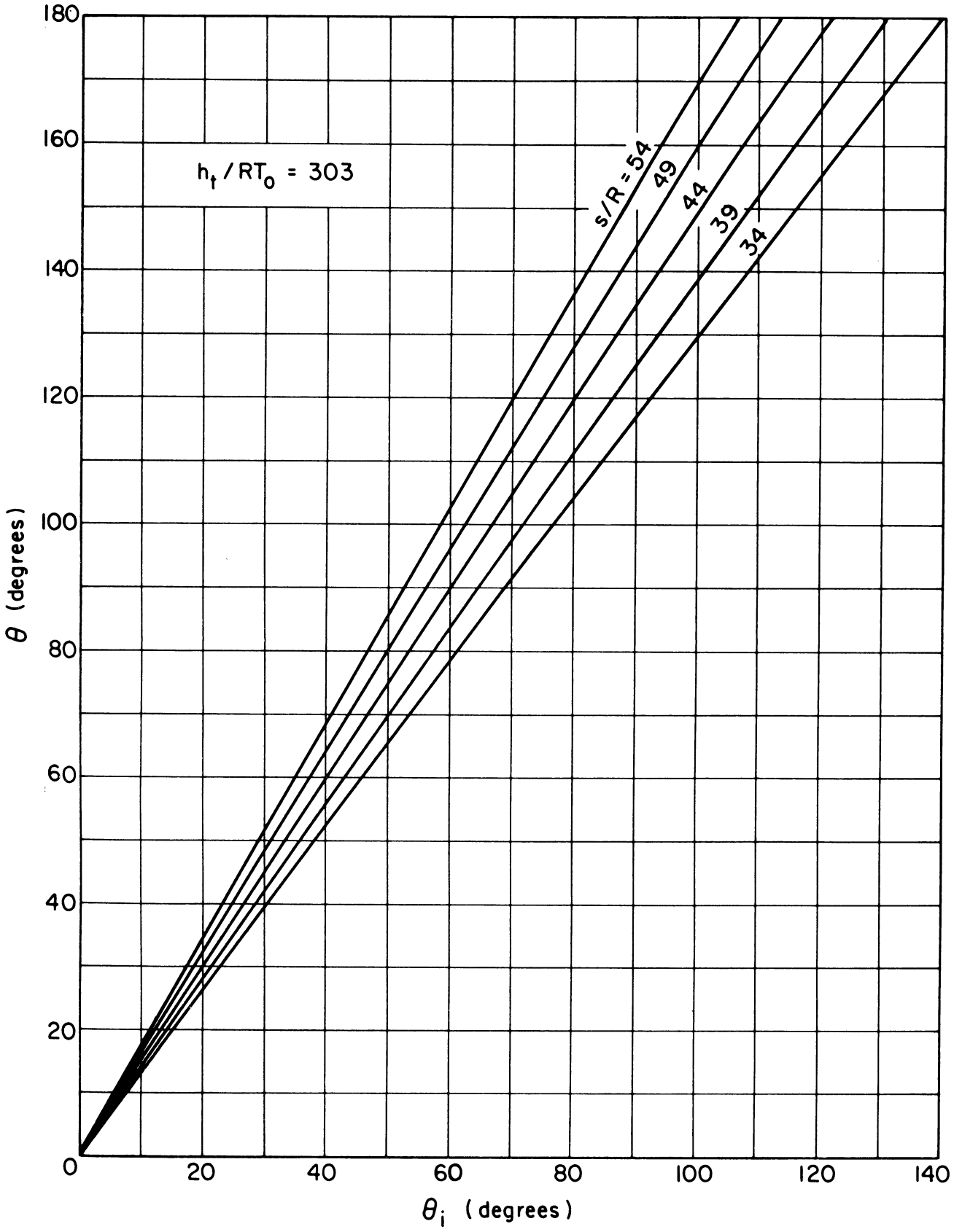

Figure 2-3. Correlation Chart A: θ vs θ_i ($h_t / RT_0 = 303$)

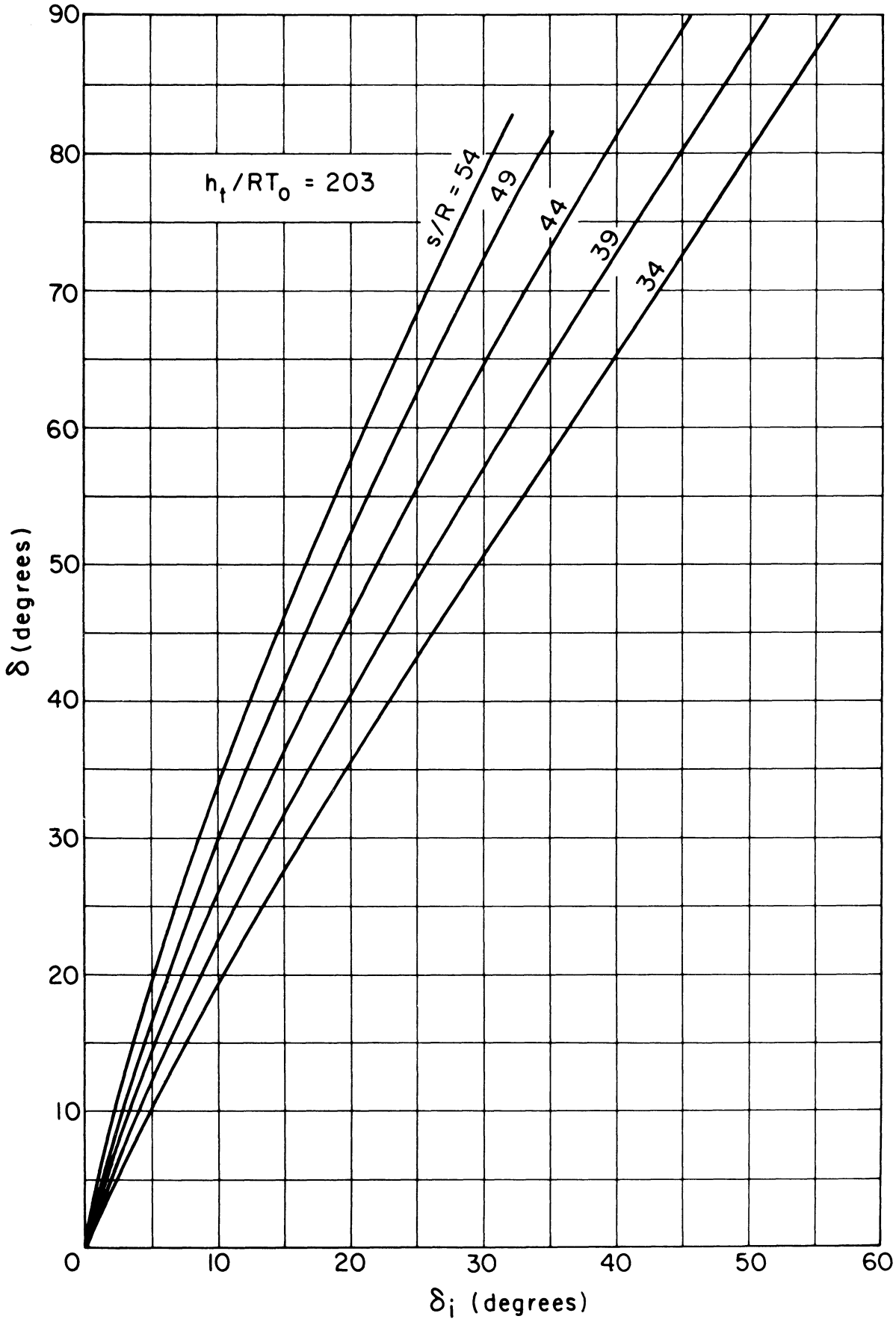

Figure 3-1. Correlation Chart B: δ vs. δ_i ($h_t/RT_0 = 203$)

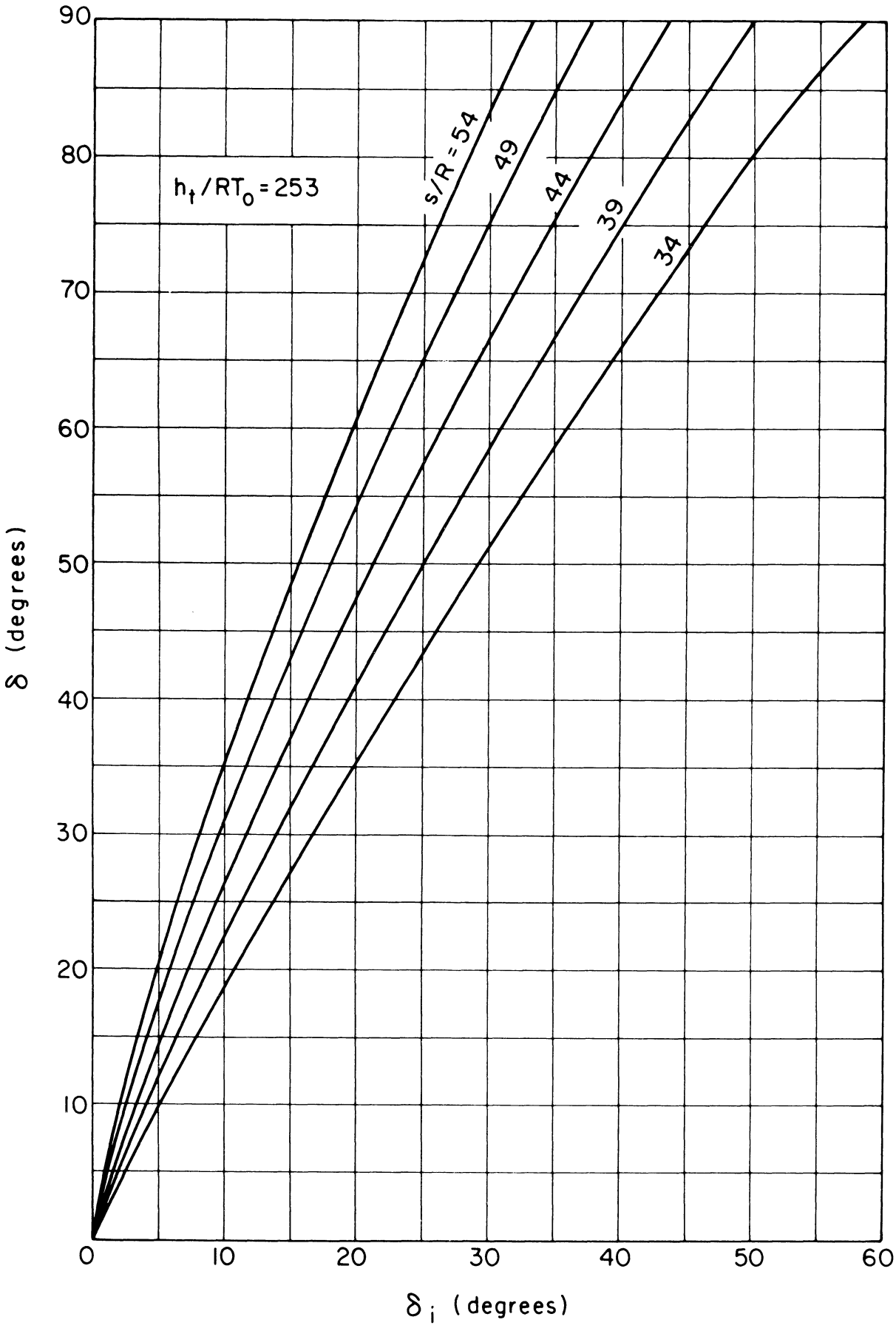

Figure 3-2. Correlation Chart B: δ vs. δ_i ($h_t/RT_0 = 253$)

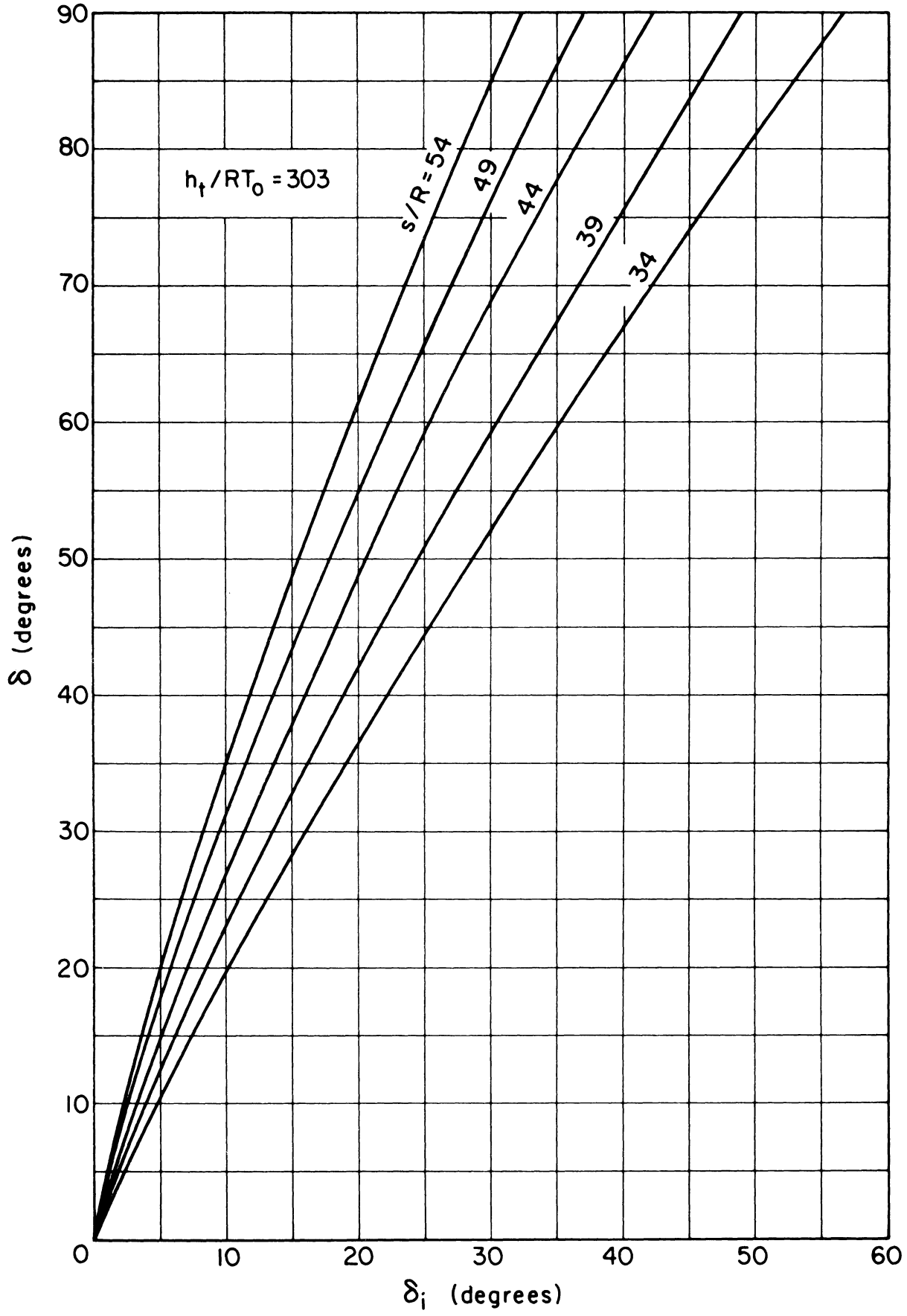

Figure 3-3. Correlation Chart B: δ vs. δ_i ($h_t / RT_0 = 303$)

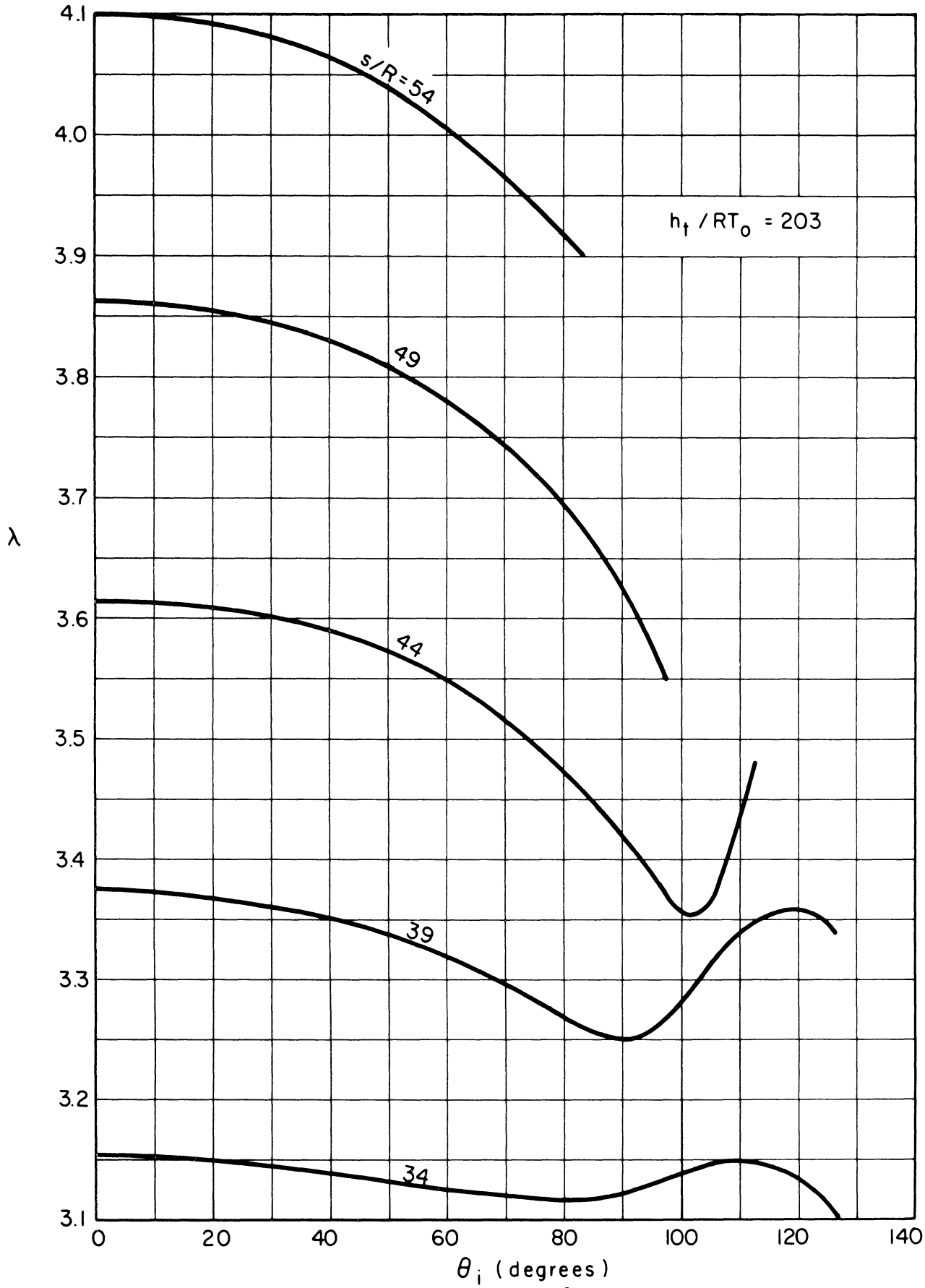

Figure 4-1. Correlation Chart C: λ vs. θ_i ($h_t / RT_0 = 203$)

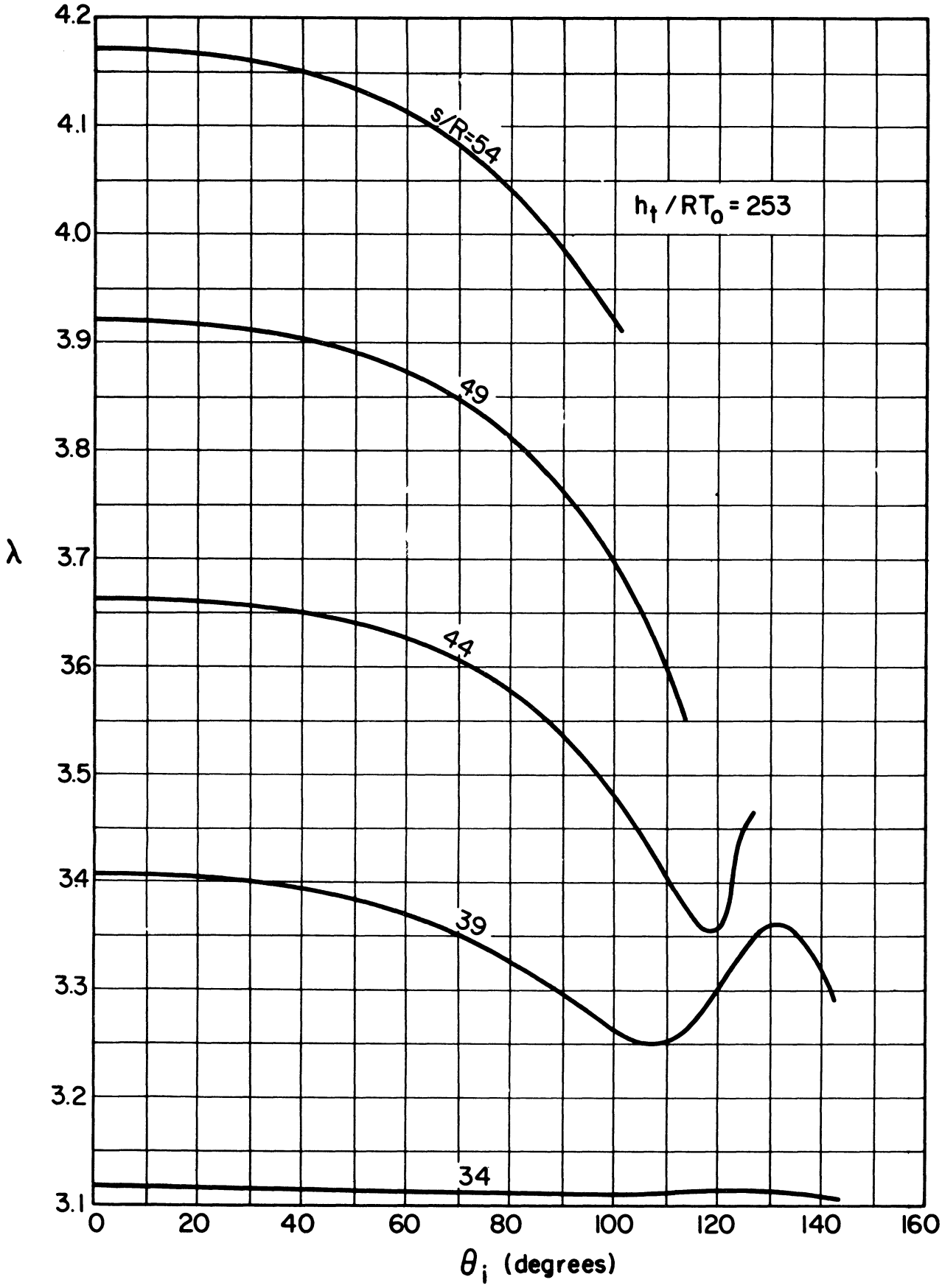

Figure 4-2. Correlation Chart C: λ vs. θ_i ($h_t/RT_0 = 253$)

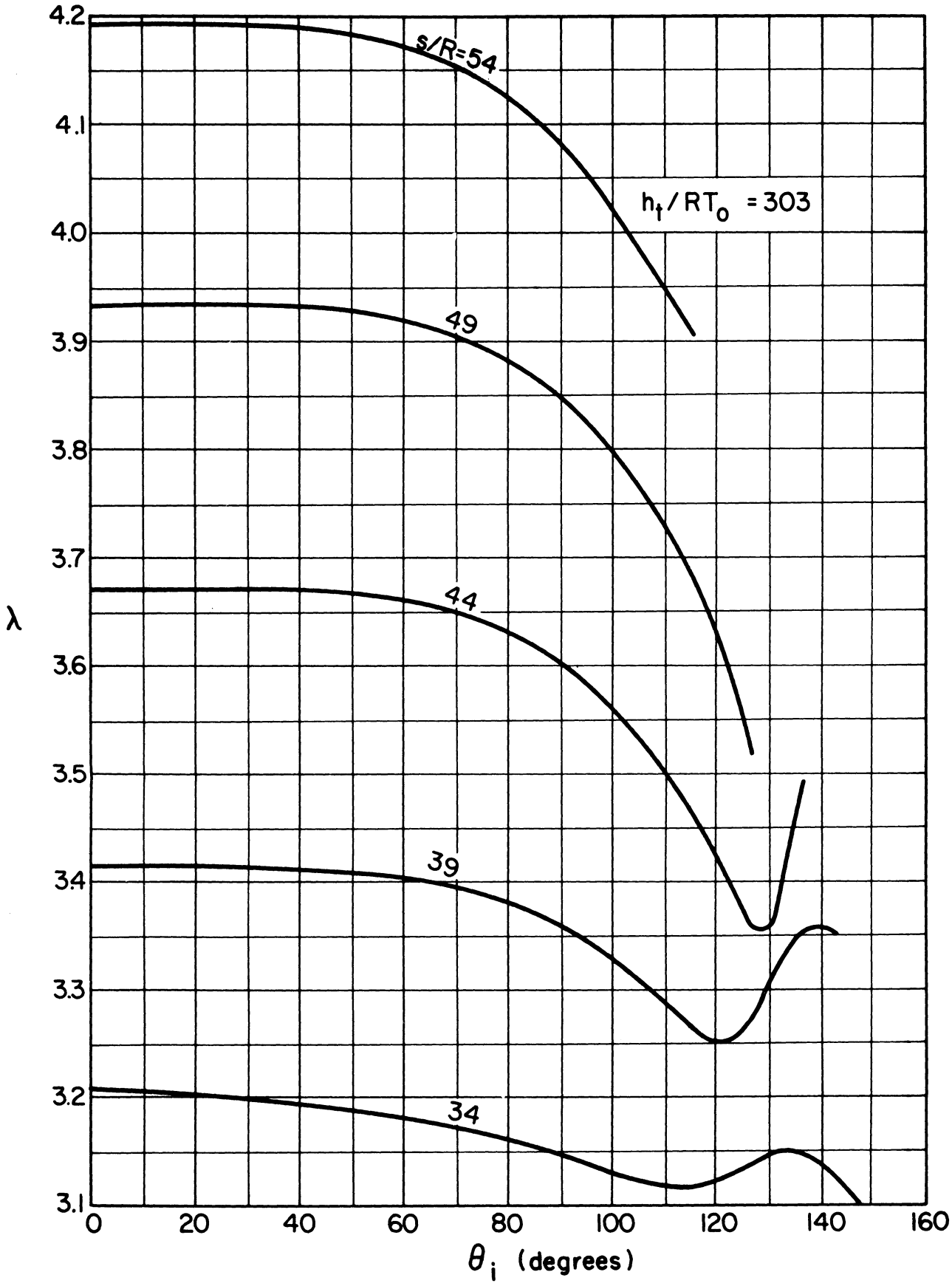

Figure 4-3. Correlation Chart C: λ vs. θ_i (h_t/RT_0 = 303)

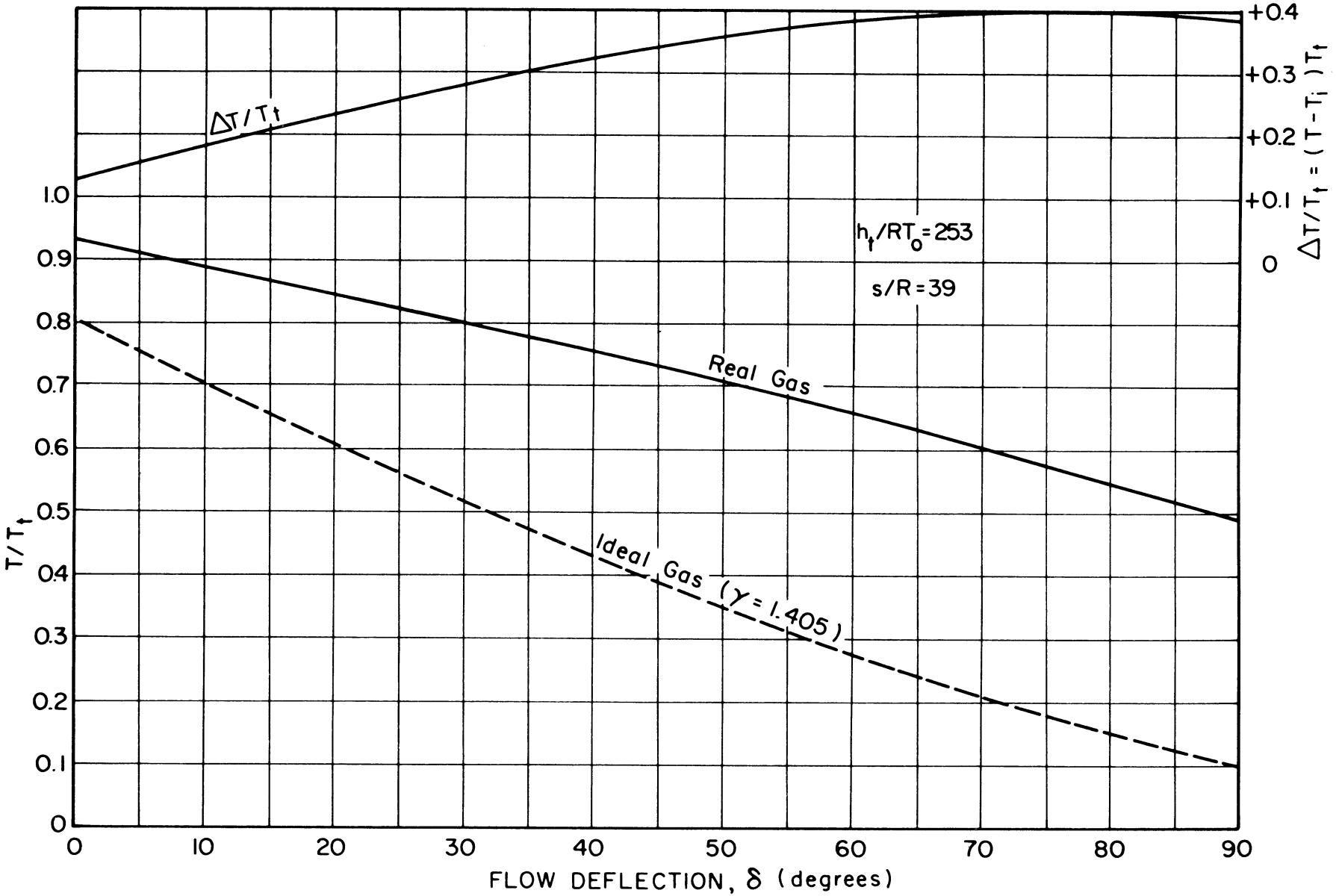

Figure 5. Temperature Variation in the Prandtl-Meyer Flow of Equilibrium Air.

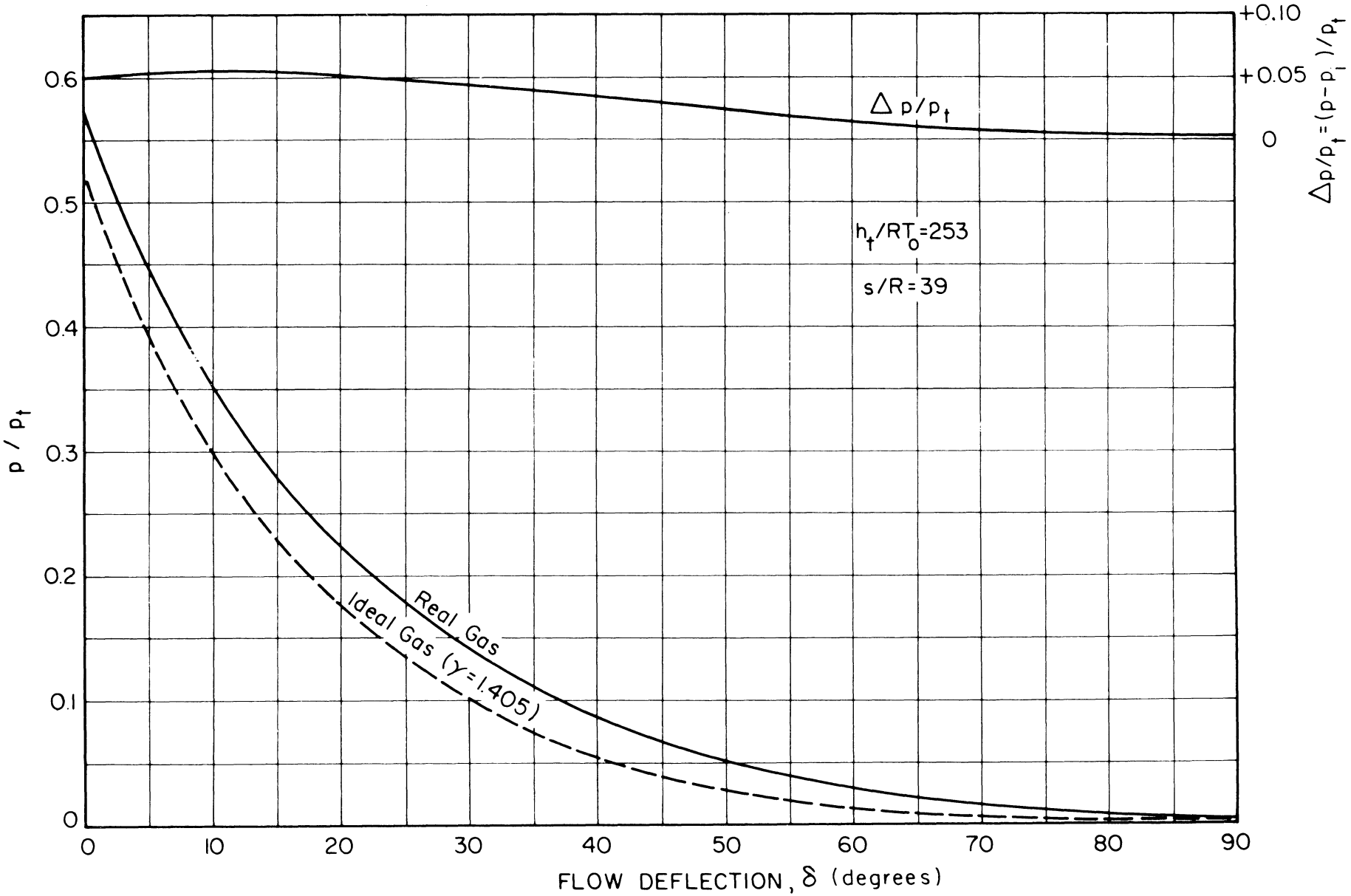

Figure 6. Pressure Variation in the Prandtl-Meyer Flow of Equilibrium Air.

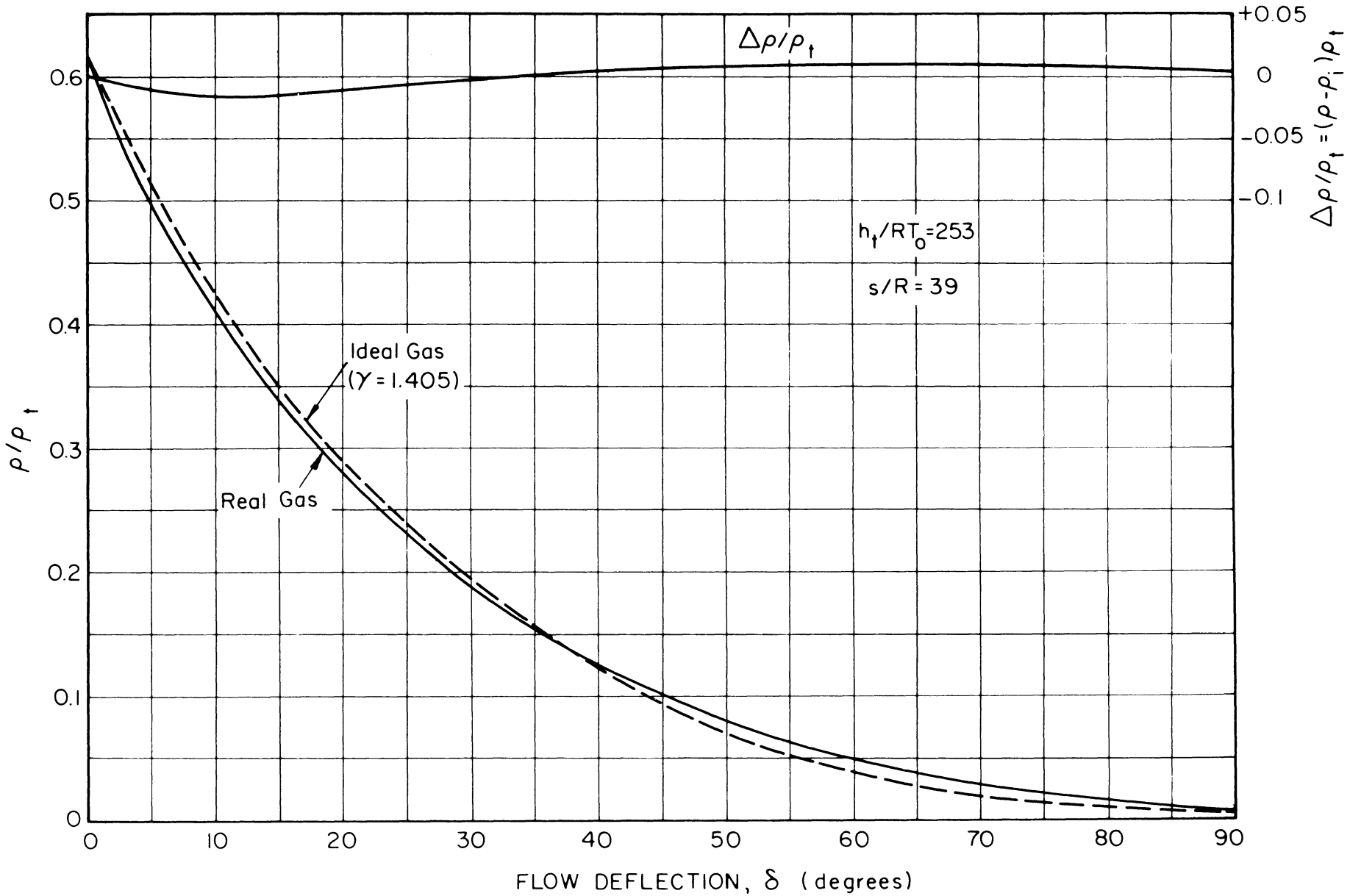

Figure 7. Density Variation in the Prandtl-Meyer Flow of Equibrium Air.

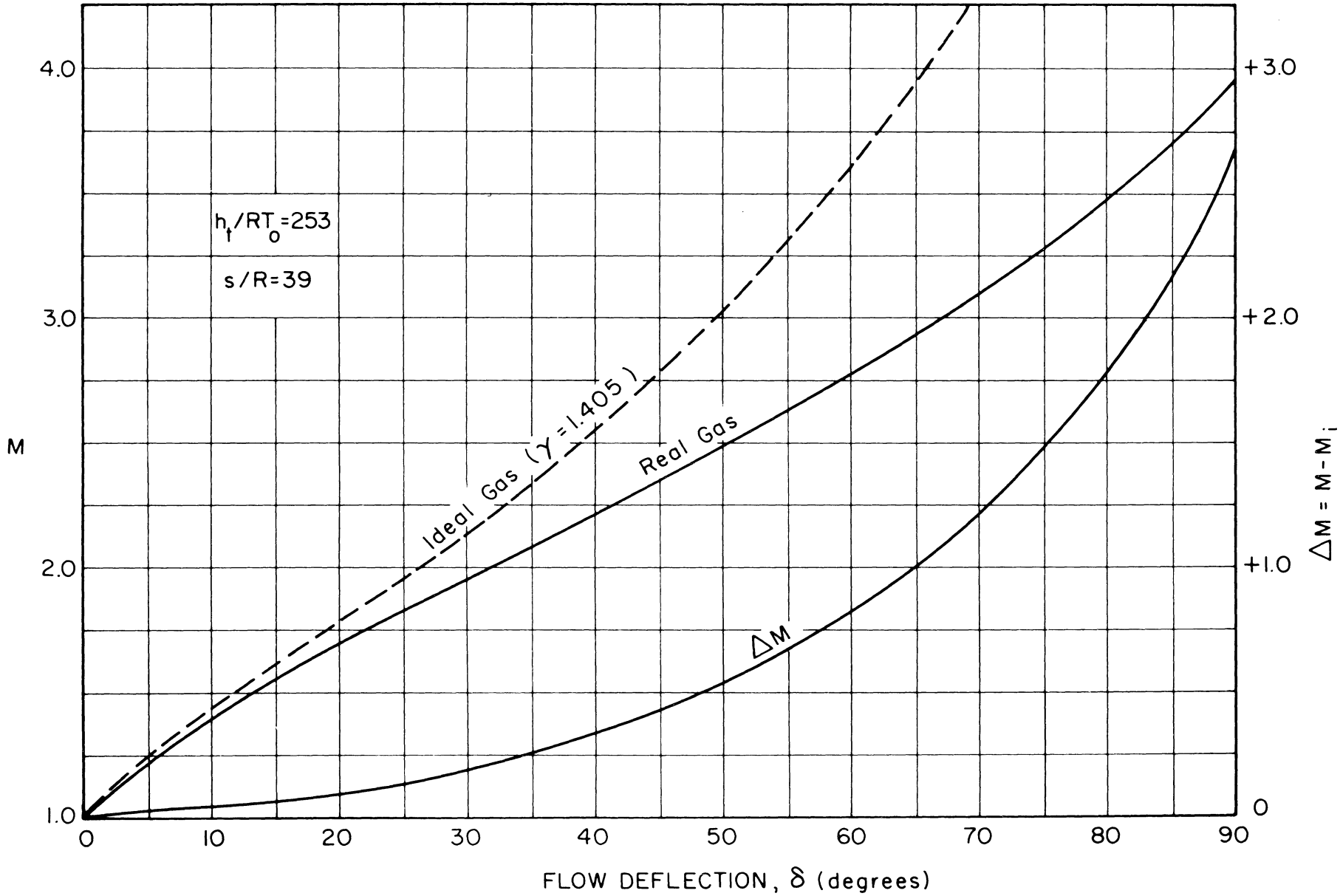

Figure 8. Mach Number Variation in the Prandtl-Meyer Flow of Equilibrium Air.

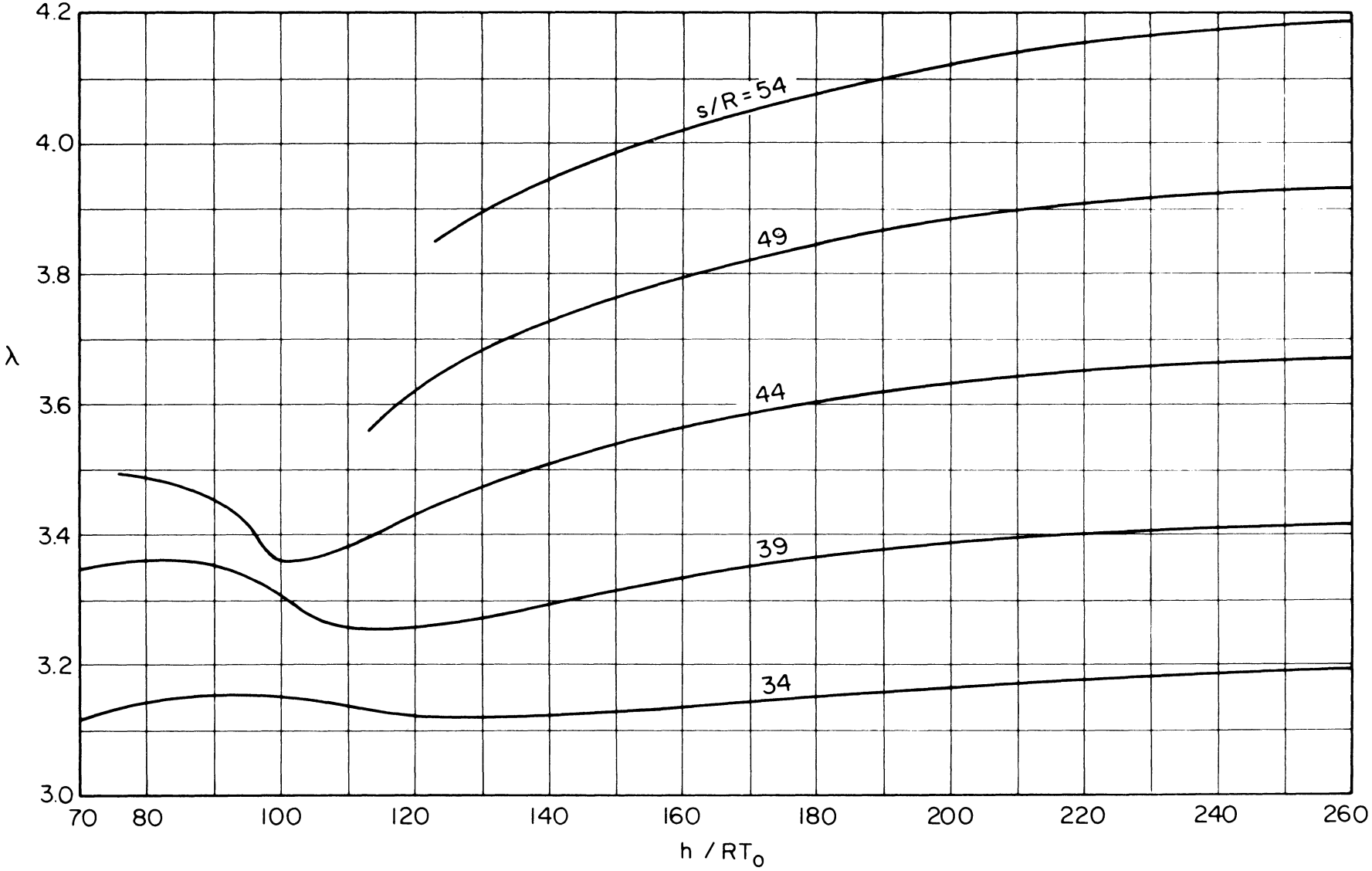

Figure 9. Variation of λ with Local Enthalpy and Entropy.

REFERENCES

1. Prandtl, L., "Neue Untersuchungen uber die stromende Bewegung der Gase und Dampfe," Phys. Zeits, 8, 23, 1907.

2. Meyer, Th., Diss. Gottingen 1908.

3. Shapiro, B., "The Dynamics and Thermodynamics of Compressible Fluid Flow," Vol. 1, 1953, pp. 474-477, 632-633.

4. Ames Research Staff, "Equations, Tables, and Charts for Compressible Flow," NACA Report 1135, 1953.

5. Lighthill, M. J., "Higher Approximations, High Speed Aerodynamics and Jet Propulsion," Vol. VI, Part E, Princton, 1954, pp. 375-377.

6. Ferri, A., "The Method of Characteristics, High Speed Aerodynamics and Jet Propulsion," Vol. VI, Part G, Princeton, 1954, pp. 591-605.

7. Sauer, Robert, "Einfuhrung in die theoretische Gasdynamik," Springer-Verlag, 1960, pp. 99-103.

8. Hilsenrath, J. and Beckett, C. W., "Tables of Thermodynamic Properties of Argon-Free Air to 15,000^{O}K," AEDC TN 56-12, National Bureau of Standards, Sept. 1956.

9. AVCO Mollier Diagram for Equilibrium Air, AVCO Research Lab. Everett,Mass., Jan. 1957.

10. Heims, S. P., "Prandtl-Meyer Expansion of Chemically Reacting Gases in Local Chemical and Thermodynamic Equilibrium," NACA TN 4230, 1958.

11. Glass, I. I. and Kawada, "Prandtl-Meyer Flow of Dissociated and Ionized Gases," Institute of Aerophysics, Univ. of Toronto, Report No. 85, 1962.

APPENDIX A

Analytical Solution for an Ideal Prandtl-Meyer Flow
Summary of Formulas*

Flow velocity, radial

$$V_r = \sqrt{2h_t} \sin \frac{\theta}{\lambda}$$

Flow velocity, transverse

$$V_\theta = \frac{\sqrt{2h_t}}{\lambda} \cos \frac{\theta}{\lambda}$$

Flow velocity, total

$$V = \frac{\sqrt{2h_t}}{\lambda} \sqrt{1 + (\lambda^2 - 1) \sin^2 \frac{\theta}{\lambda}}$$

Flow velocity, dimensionless

$$M^* = \sqrt{1 + (\lambda^2 - 1) \sin^2 \frac{\theta}{\lambda}}$$

Mach number

$$M = \sqrt{1 + \lambda^2 \tan^2 \frac{\theta}{\lambda}}$$

Mach angle

$$\alpha = \tan^{-1} \frac{1}{\lambda} \cot \frac{\theta}{\lambda}$$

Deflection angle

$$\delta = \theta - \tan^{-1} \lambda \tan \frac{\theta}{\lambda}$$

Temperature

$$T = T_t \left(1 - \frac{1}{\lambda^2}\right) \cos^2 \frac{\theta}{\lambda}$$

Enthalpy

$$h = h_t \left(1 - \frac{1}{\lambda^2}\right) \cos^2 \frac{\theta}{\lambda}$$

Pressure

$$p = p_t \left[\left(1 - \frac{1}{\lambda^2}\right) \cos^2 \frac{\theta}{\lambda}\right]^{\frac{1}{2}(\lambda^2 + 1)}$$

Density

$$\rho = \rho_t \left[\left(1 - \frac{1}{\lambda^2}\right) \cos^2 \frac{\theta}{\lambda}\right]^{\frac{1}{2}(\lambda^2 - 1)}$$

Flow parameter

$$\lambda \equiv \sqrt{\frac{\gamma + 1}{\gamma - 1}}$$

---

*For simplicity, all subscripts (i) for ideal flow have been omitted.

APPENDIX B

A Short Table for the Prandtl-Meyer Flow of an Ideal Diatomic Gas ($\gamma = 1.405$)*

δ [°]	θ [°]	α [°]	p/p_t	M	M*	T/T_t
0	0,00	90,00	0,527	1,000	1,000	0,832
1	23,72	67,28	0,477	1,084	1,068	0,808
2	30,04	61,96	0,449	1,133	1,107	0,794
3	34,82	58,18	0,424	1,178	1,141	0,781
4	38,88	55,12	0,401	1,220	1,173	0,768
5	42,34	52,66	0,381	1,258	1,201	0,757
6	45,42	50,58	0,363	1,295	1,227	0,747
7	48,30	48,70	0,345	1,332	1,253	0,736
8	50,93	47,07	0,329	1,366	1,276	0,726
9	53,46	45,54	0,313	1,401	1,299	0,716
10	55,84	44,16	0,298	1,435	1,322	0,706
11	58,16	42,84	0,284	1,470	1,344	0,696
12	60,38	41,62	0,270	1,505	1,366	0,686
13	62,49	40,51	0,257	1,539	1,387	0,676
14	64,52	39,48	0,245	1,572	1,407	0,667
15	66,53	38,47	0,233	1,608	1,428	0,657
16	68,47	37,53	0,221	1,641	1,448	0,647
17	70,33	36,67	0,210	1,675	1,467	0,638
18	72,18	35,82	0,199	1,710	1,486	0,628
19	73,98	35,02	0,189	1,744	1,504	0,619
20	75,74	34,26	0,179	1,779	1,523	0,609
21	77,49	33,51	0,170	1,815	1,541	0,600
22	79,20	32,80	0,161	1,850	1,559	0,591
23	80,90	32,10	0,153	1,884	1,576	0,582
24	82,55	31,45	0,145	1,918	1,592	0,573
25	84,20	30,80	0,137	1,954	1,609	0,564
26	85,81	30,19	0,130	1,989	1,625	0,555
27	87,42	29,58	0,123	2,025	1,641	0,546
28	89,02	28,98	0,116	2,062	1,657	0,537
29	90,58	28,42	0,110	2,098	1,673	0,529
30	92,12	27,88	0,104	2,135	1,688	0,520
31	93,66	27,34	0,097	2,174	1,704	0,511
32	95,18	26,82	0,092	2,214	1,720	0,502
33	96,68	26,32	0,086	2,251	1,735	0,493
34	98,20	25,80	0,080	2,296	1,752	0,483
35	99,67	25,33	0,075	2,339	1,767	0,474
36	101,13	24,87	0,071	2,378	1,781	0,466
37	102,58	24,42	0,066	2,422	1,795	0,457
38	104,02	23,98	0,062	2,466	1,810	0,448
39	105,46	23,54	0,058	2,508	1,824	0,440
40	106,88	23,12	0,054	2,550	1,837	0,432
41	108,30	22,70	0,051	2,595	1,851	0,423
42	109,71	22,29	0,047	2,640	1,864	0,415
43	111,11	21,89	0,044	2,689	1,878	0,406
44	112,51	21,49	0,041	2,734	1,891	0,398
45	113,89	21,11	0,038	2,778	1,903	0,390
46	115,27	20,73	0,036	2,826	1,917	0,382
47	116,63	20,37	0,033	2,873	1,928	0,374
48	118,00	20,00	0,031	2,920	1,939	0,367
49	119,36	19,64	0,029	2,968	1,951	0,359
50	120,71	19,29	0,027	3,021	1,963	0,351
51	122,07	18,93	0,025	3,074	1,975	0,343
52	123,41	18,59	0,023	3,131	1,987	0,335
53	124,74	18,26	0,021	3,188	1,999	0,327
54	126,03	17,97	0,019	3,350	2,012	0,319
129,32	219,32	0,00	0,000	∞	2,437	0,000

(Taken from Ref. 7, p. 102)

*For simplicity, all subscripts (i) for ideal flow have been omitted.

APPENDIX C

An Empirical Formula for the θ vs. θ_i Relation for Equilibrium Air

As shown in Figs. 2-1 to 2-3 the θ vs. θ_i relations for equilibrium air are nearly linear under the given stagnation conditions. Such a relation may be approximated by

$$\theta = \frac{\bar{\lambda}}{\lambda_i} \theta_i \tag{C-1}$$

where $\bar{\lambda}$ is the average λ over the range of plotting. The value of $\bar{\lambda}$ may be obtained either from the λ vs. θ_i curve, or by directly measuring the average slope of the θ vs. θ_i curve. By so doing we find that $\bar{\lambda}$ is strongly dependent on s/R, and only weakly dependent on h_t/RT_o, either dependence being also nearly linear. An empirical formula is found to be

$$\frac{\bar{\lambda}}{\lambda_i} = 0.633 + .0172\,(s/R) - 2.00\,(10)^{-4}\,(h_t/RT_o) + 1.20\,(10)^{-5}\,(h_t/RT_o)\,(s/R) \tag{C-2}$$

which holds approximately for equilibrium air within the following range of stagnation conditions:

$$h_t/RT_o = 203 \text{ to } 303$$

$$s/R = 34 \text{ to } 59$$

APPENDIX D

Numerical Examples

1. Equilibrium air is approaching a convex sharp corner at a Mach number of 1 under the stagnation condition:

$$\frac{h_t}{RT_o} = 253 \quad , \quad \frac{s}{R} = 39$$

Find the Mach number, temperature, and pressure of the gas along the radial line inclined at 10^o from the initial flow direction as shown in Fig. D-1. Find also the local flow deflection.

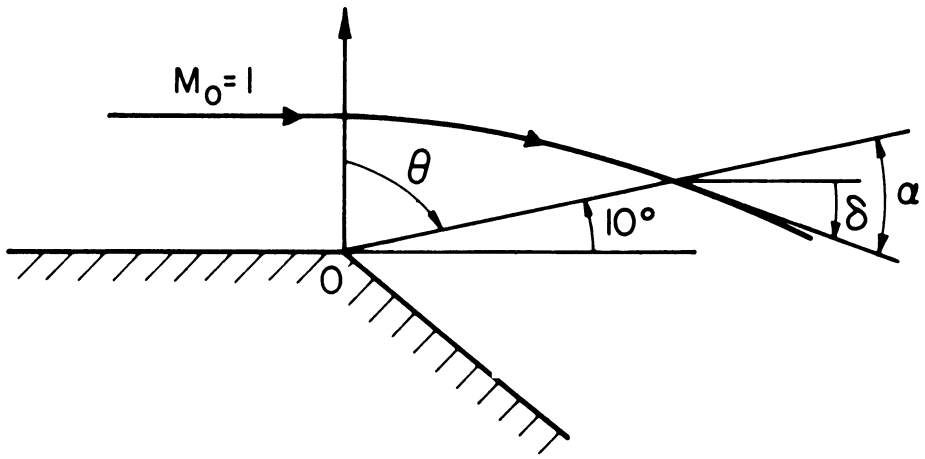

Figure D-1. Example 1.

Solution: The polar angle of the radial line is

$$\theta = 90^o - 10^o = 80^o$$

From the correlation chart A (Fig. 2-2) we find

$$\theta_i = 58.5^o$$

The analytical solution of the ideal flow at this polar angle is found from Appendix B (or A) to be

$$M_i = 1.475 \quad , \quad \frac{h_i}{h_t} = \frac{T_i}{T_t} = 0.6945 \quad , \quad \delta_i = 11.15$$

The local value of λ as found from Fig. 4-2 is

$$\lambda = 3.372 \quad \text{or} \quad \lambda^2 = 11.37$$

The value of λ for an ideal gas (diatomic) is

$$\lambda_i = \sqrt{6} \quad \text{or} \quad \lambda_i^2 = 6$$

The local Mach number in the real flow, according to formula (11) is given by

$$M^2 = 1 + \frac{11.37}{6}(1.475^2 - 1) = 3.228$$

$$M = 1.796$$

The ideal local enthalpy is given by

$$\frac{h_i}{RT_o} = \left(\frac{h_i}{h_t}\right)\left(\frac{h_t}{RT_o}\right) = (0.6945)(253) = 175.7$$

The local enthalpy in the real flow is then calculated from correlation formula (12):

$$\frac{h}{h_i} = \frac{1 - \frac{1}{11.37}}{1 - \frac{1}{6}} = 1.094$$

$$\frac{h}{RT_o} = \frac{h}{h_i}\left(\frac{h_i}{RT_o}\right) = (1.094)\,(175.7) = 192.2$$

The corresponding temperature and pressure are then found from the Mollier chart[9]:

$$T = 6725^{o}k \qquad p = 13.0 \text{ atm}$$

To find the local flow deflection we first calculate

$$\sin \alpha = \frac{1}{M} = \frac{1}{1.796} = 0.5568 \quad , \quad \alpha = 33^{o}\ 50'$$

Then by Eq. (13) we find

$$\delta = \theta + \alpha - \frac{\pi}{2} = 80^{o} + 33^{o}\ 50' - 90^{o} = 23^{o}\ 50'$$

The value of δ could also be found from the δ vs. δ_i chart (Fig. 3-2).

2. For the flow of example 1 find the Mach number, temperature, and pressure of the gas when the local flow deflection is 60^{o}.

Solution: The ideal flow deflection corresponding to $\delta = 60^{o}$ is found from correlation chart B (Fig. 3-2).

$$\delta_i = 31^{o}$$

and theideal gassolution (Appendix A or B) gives

$$M_i = 2.174 \quad , \quad \frac{h_i}{h_t} = \frac{T_i}{T_t} = 0.511 \quad , \quad \theta_i = 93.66^{\circ}$$

The value of λ is then found from Fig. 4-2.

$$\lambda = 3.287$$

By using the correlation formulas (11) and (12) we calculate for the real flow,

$$M^2 = 1 + \frac{3.287^2}{6}(2.174^2 - 1) = 7.711 \quad , \quad M = 2.777$$

$$\frac{h}{h_i} = \frac{1 - \frac{1}{3.287^2}}{1 - \frac{1}{6}} = 1.089$$

The local enthalpy in the real flow is thus given by

$$\frac{h}{RT_o} = \left(\frac{h}{h_i}\right)\left(\frac{h_i}{h_t}\right)\left(\frac{h_t}{RT_o}\right) = (1.089)\,(0.511)\,(253) = 140.8$$

From the Mollier chart we find

$$T = 5350^{\circ}K \quad , \quad p = 2.19 \text{ atm}$$

3. Same as example 1 except that the air is approaching the sharp corner at Mach number 2.

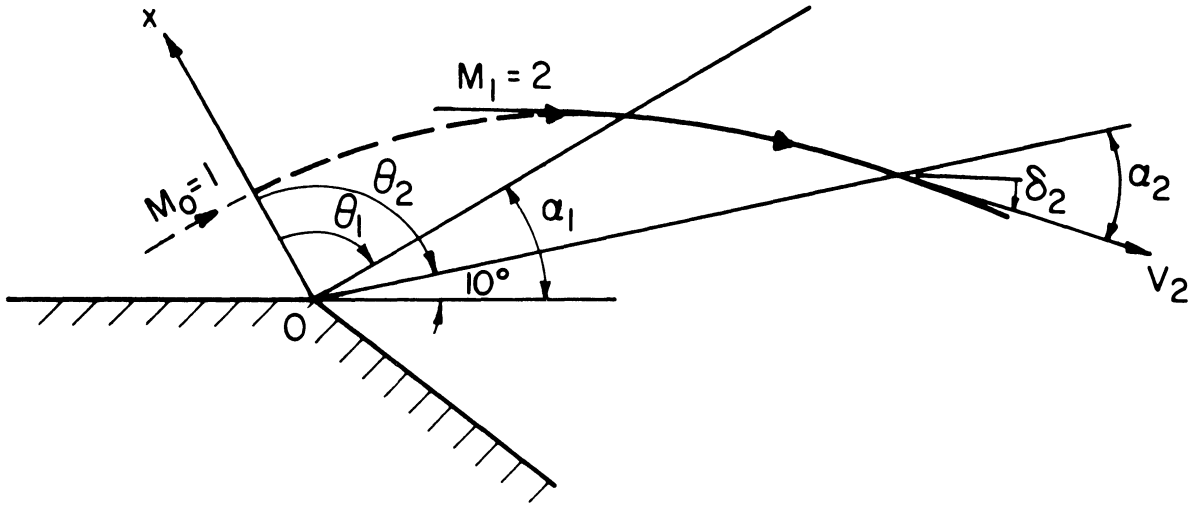

Figure D-2. Example 2.

Solution: To start the calculation the local enthalpy of the air at the initial Mach number ($M_1 = 2$) must be determined. This can be done graphically with the help of the Mollier chart[9] as follows:

Assume a series of values of h/RT_o ($< h_t/RT_o$) and find the corresponding value of "a" along the constant entropy line ($s/R = 39$) in the Mollier chart; calculate the flow velocity V from the energy equation $V = \sqrt{2\,(h_t - h)}$ and then the Mach number $M = V/a$; finally plot M vs. h and thus find from the graph the value of h at the given Mach number ($M_1 = 2$).

For the present problem the result of such a plotting is shown in Fig. D-3, from which

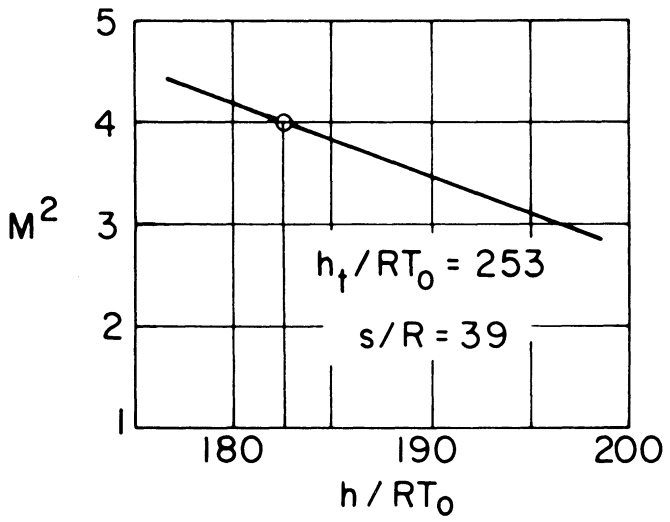

Figure D-3. Isentropic Variation of Mach Number with Local Enthalpy.

From which we find

$$\frac{h_1}{RT_o} = 182.5$$

while the corresponding speed of sound is given by the Mollier chart[9]

$$\frac{a_1}{a_o} = 5.025$$

The initial value of the parameter λ is thus found from Eq. (4) or Fig. 9,

$$\lambda_1 = 3.366$$

The initial ideal polar angle is then found from Eq. (15), or Fig. 4-2,

$$(\theta_1)_i = 62^o$$

and the corresponding polar angle, found from the correlation chart A (Fig. 2-2),

$$\theta_1 = 85^\circ$$

which, as we understand, is measured from the fictitious Mach line M = 1.

To find the polar angle of the 10° radial line we first calculate

$$\alpha_1 = \sin^{-1}\frac{1}{M_1} = \sin^{-1}\frac{1}{2} = 30^\circ$$

and then from the geometry of the flow (see Fig. D-2) we find

$$\theta_2 = \theta_1 + \alpha_1 - 10^\circ = 85^\circ + 30^\circ - 10^\circ = 105^\circ$$

From now on the procedures are the same as thos in example 1.

The results are as follows:

Ideal flow:	$(\theta_2)_i = 77^\circ$	(Fig. 2-2)
	$(M_2)_i = 1.805$	(Ideal solution, Appendix A or B)
	$(h_2)_i/h_t = 0.603$	(ditto)
Real flow:	$\lambda_2 = 3.335$	(Fig. 4-2)
	$M_2 = 2.277$	(Eq. (11))
	$h_2/RT_o = 166.6$	(Eq. (12))
	$T_2 = 6100^\circ K$	(Mollier chart[9])

$$p_2 = 5.96 \text{ atm} \qquad \text{Mollier chart}^{9}$$

$$\alpha_2 = \sin^{-1}\frac{1}{M_2} = 26^{\circ}\ 3'$$

The flow deflection measured from the initial flow direction at $M_1 = 2$ is, from the geometry in Fig. D-2,

$$\delta_2' = 26^{\circ}\ 3' - 10^{\circ} = 16^{\circ}\ 3'$$

4. For the flow of example 3, find the Mach number, temperature, and pressure of the gas when the local flow deflection is 60° from the initial flow direction at $M_1 = 2$.

Solution: From example 3 we have

$$\theta_1 = 85^{\circ} \quad , \quad \alpha_1 = 30^{\circ}$$

The initial flow deflection measured from the fictitious flow M = 1 is, by Eq. (13),

$$\delta_1 = 85^{\circ} + 30^{\circ} - 90^{\circ} = 25^{\circ}$$

The corresponding local flow deflection is

$$\delta_2 = 25^{\circ} + 60^{\circ} = 85^{\circ}$$

From now on the procedures are the same as those in example 2. The results are as follows:

Ideal flow: $(\delta_2)_i = 46.7$ (Fig. 3-2)

$(M_2)_i = 2.859$ (Appendix A or B)

$h_{2i}/h_t = T_{2i}/T_t = 0.376$ (ditto)

$\theta_{2i} = 116.2$ (ditto)

Real flow: $\lambda_2 = 3.291$ (Fig. 4-2)

$M_2 = 3.72$ (Eq. (11))

$h_2/RT_o = 103.5$ (Eq. (12))

$T_2 = 3990^oK$ (Mollier chart[9])

$p_2 = 0.288$ atm (ditto)